

Computation of Static, Steady-state and Dynamic Characteristics of the Switched Reluctance Motor

UDK 621.313.13
 IFAC IA 4.6.1

Original scientific paper

This paper gives an overview of the procedures of determination of static characteristics (flux linkage, magnetic coenergy and torque), steady state characteristics (current and torque) and dynamic characteristics (speed, current and torque) of switched reluctance motor. A two dimensional distribution of magnetic vector potential inside a motor is computed using finite element method. The flux linkage, magnetic coenergy and static torque are calculated for different rotor positions and stator currents. Steady-state and dynamic characteristics are calculated using specially developed software routines. All calculations are realized for switched reluctance motor with 8 stator and 6 rotor poles. Numerically obtained results are verified by experiment.

Key words: switched reluctance motor, characteristics, modelling

1 INTRODUCTION

The switched reluctance (SR) motor is an electric motor in which torque is produced by the tendency of its rotor to move to a position where the inductance of the excited winding is maximized. The SR motor consists of a salient pole stator with concentrated excitation windings and a salient pole rotor with no conductors or permanent magnets.

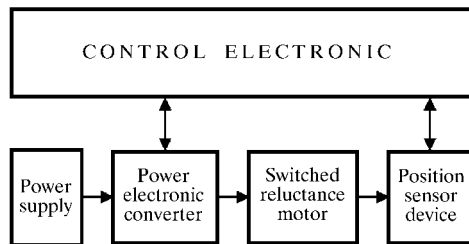


Fig. 1 The basic structure of the switched reluctance drive

The switched reluctance machine, its power electronic converter, control unit and the rotor position sensing device form the switched reluctance drive system as shown in Figure 1. The list of publication concerned with switched reluctance drives is very long and spans the period from 1979 until now. Several references which deal with the principles of switched reluctance drives are listed [1-6]. This paper gives an overview of procedures for prediction of SR motor waveforms referred to as the static characteristics (current and torque vs. position) and dynamic characteristics (speed, current and torque vs. time). Figure 1 shows the basic structure of the switched reluctance drive.

The relationship between stator phase current and torque in switched reluctance motor are highly nonlinear and the performance of the switched reluctance motor cannot be modelled using simple analytic functions and equivalent circuits. The proper evaluation of the motor design and performance and the optimization of a switched reluctance motor requires magnetic analysis in the whole transversal section for a range angular position of the rotor and winding current supply sequence. The computation of the flux linkage of one phase of the switched reluctance motor, as a function of rotor position and phase current, is the first step in performance prediction of the switched reluctance

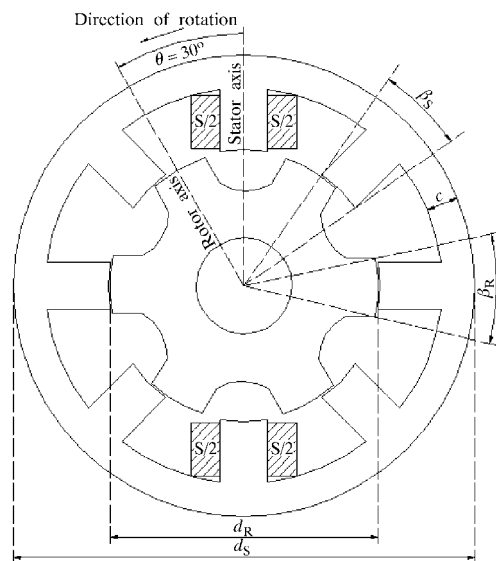


Fig. 2 SR motor cross section

motor. For that, magnetic field equations must be solved, taking into account saturation effects of stator and rotor material.

This paper describes the procedures of determination of static characteristics using finite element method and steady-state and dynamic characteristics using appropriate mathematical model for SR motor with 8 stator and 6 rotor poles and with bifilar winding supplied from power electronic converter.

The SR motor cross section with designation of main geometry dimensions is shown in Figure 2. The numerical values are given in appendix.

2 STATIC CHARACTERISTICS

The static characteristics of SR motor are defined as look-up table flux linkage $\Psi(\theta, i)$, magnetic coenergy $W_{co}(\theta, i)$ and electromagnetic torque $T(\theta, i)$ for one motor's phase. These characteristics are computed and measured for range of rotor position θ and phase current i with blocked rotor. The computation of the static characteristics is the first step in the performance prediction of the SR motor.

2.1 Flux linkage

The flux linkage look-up table $\Psi(\theta, i)$ can be determined by using finite element method (FEM), e.g. computing the scalar values of the magnetic vector potential \vec{A} over the motor cross section (Figure 2). The resulting scalar values of calculated distribution of magnetic vector potential were post-processed to produce the values of flux linkage as shown in [7]:

$$\Psi(\theta, i) = \frac{l}{I} \int_V \vec{J} \cdot \vec{A} dV = \frac{N_{PH} \cdot l}{S} \sum_{k=1}^n A_k \cdot S_k, \quad (1)$$

where are: I – winding excitation current, \vec{J} – source current density, \vec{A} – magnetic vector potential, N_{PH} – number of turns per phase windings, l – machine axial length, S – area for phase winding, A_k and S_k – scalar values of magnetic vector potential and area of the k^{th} elements, n – number of elements in the area.

Two dimensional magnetostatic problem of computation scalar values of the magnetic vector potential \vec{A} in Cartesian coordinates (x, y) is described by the nonlinear Poisson's equation:

$$\frac{\partial}{\partial x} \left(\nu(B) \cdot \frac{\partial A}{\partial x} \right) + \frac{\partial}{\partial y} \left(\nu(B) \cdot \frac{\partial A}{\partial y} \right) = -J(x, y), \quad (2)$$

where are: $\nu(B)$ – the magnetic reluctivity, J – scalar value current density.

The magnetic vector potential must be solved taking into account saturation effects of the ferromagnetic material of stator and rotor (Figure 3).

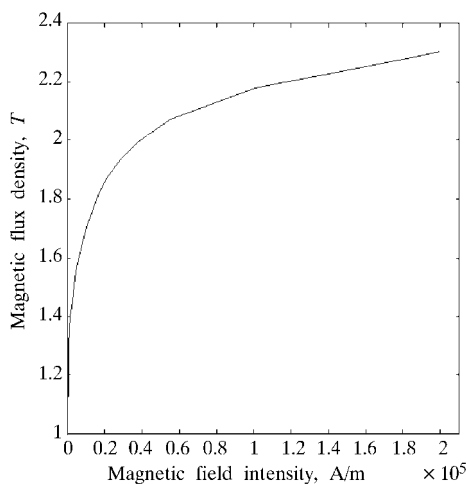


Fig. 3 $B = f(H)$ characteristic of stator and rotor material of the SR motor

Solving equation (2) on model of SR motor discretized for FEM analysis (Figure 4) were made with a range of angular displacements from -30° to 30° , in 3° increments and for different excitation currents.

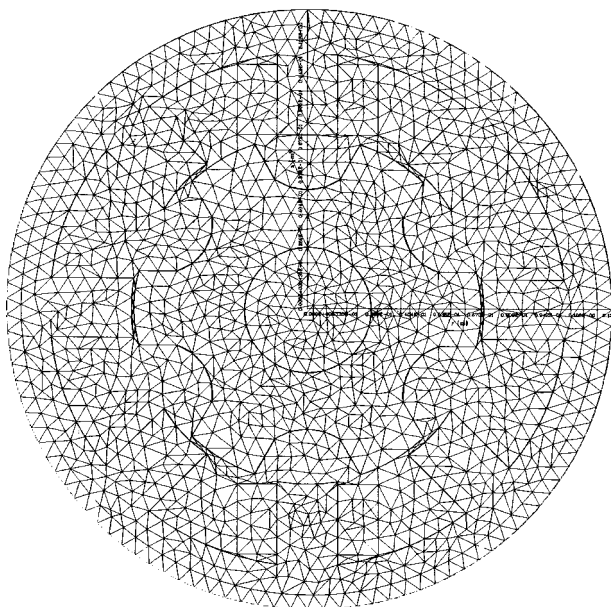


Fig. 4 Discretized model of SR motor

Figure 5, 6 and 7 shows distribution of magnetic vector potential \vec{A} for three different rotor position: unaligned position with -30° , position with -9° and aligned position with 0° of angular displacement between stator axes and rotor poles.

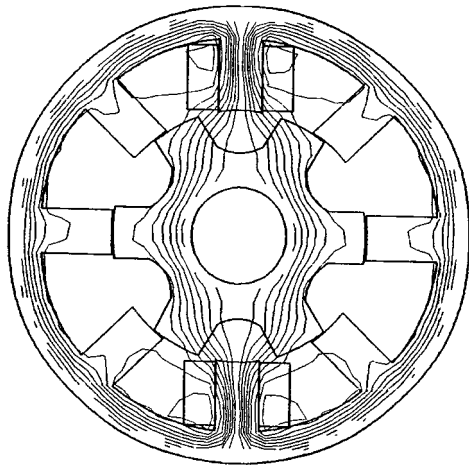


Fig. 5 Distribution of vector potential \vec{A} in unaligned position ($\theta = -30^\circ$)

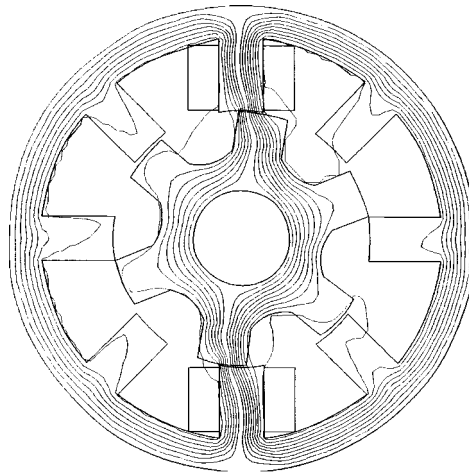


Fig. 6 Distribution of vector potential \vec{A} in position $\theta = -9^\circ$ between stator axes and rotor poles

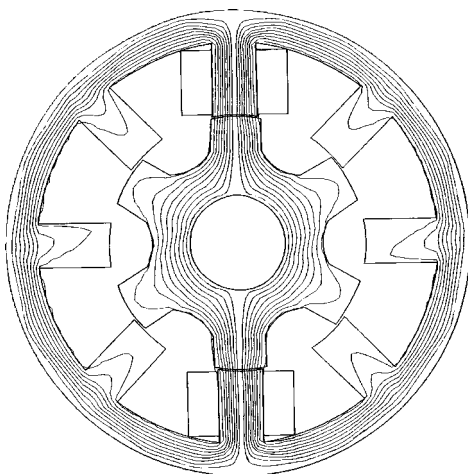


Fig. 7 Distribution of vector potential \vec{A} in aligned position ($\theta = 0^\circ$)

Figure 8 shows flux linkage $\Psi(\theta, i)$ as a function of displacement angle and winding excitation current. The cubic spline interpolation is used to determine the intermediate values.

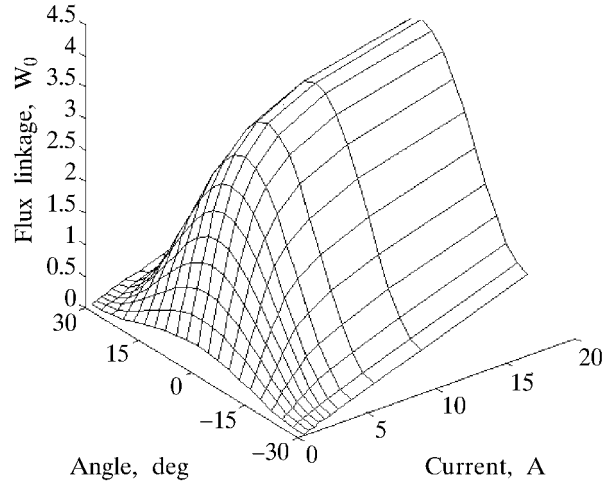


Fig. 8 Computed characteristics of the flux linkage $\Psi(\theta, i)$

2.2 Magnetic coenergy

Magnetic coenergy $W_{co}(\theta, i)$ can be calculated on the basis of flux linkage $\Psi(\theta, i)$ characteristics using methods of numerical derivation as:

$$W_{co}(\theta, i) = \int_0^i \Psi(\theta, i) di \Big|_{i=\text{const}} \quad (3)$$

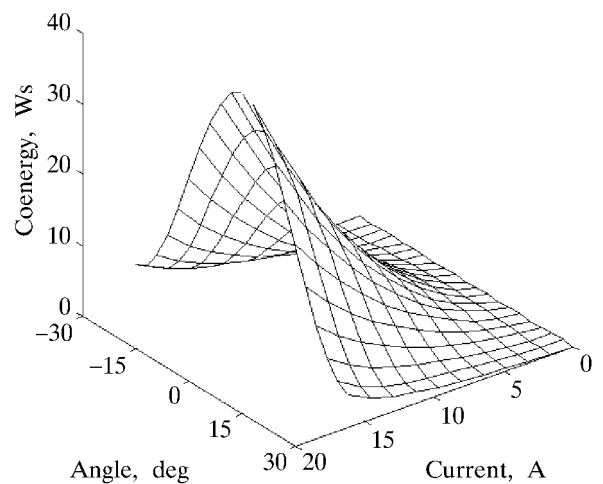


Fig. 9 Magnetic coenergy characteristics $W_{co}(\theta, i)$

The coenergy as a function of displacement angle and winding excitation current is shown in Figure 9.

2.3 Electromagnetic torque

The electromagnetic torque $T(\theta, i)$ was calculated from the derivative of the coenergy curves with respect to the angular displacement θ using methods of numerical derivation for different rotor positions and winding excitation current:

$$T(\theta, i) = \left. \frac{\partial W_{co}(\theta, i)}{\partial \theta} \right|_{i=\text{const}} \quad (4)$$

The electromagnetic torque for a one phase as a function of displacement angle and winding excitation current is shown in Figure 10.

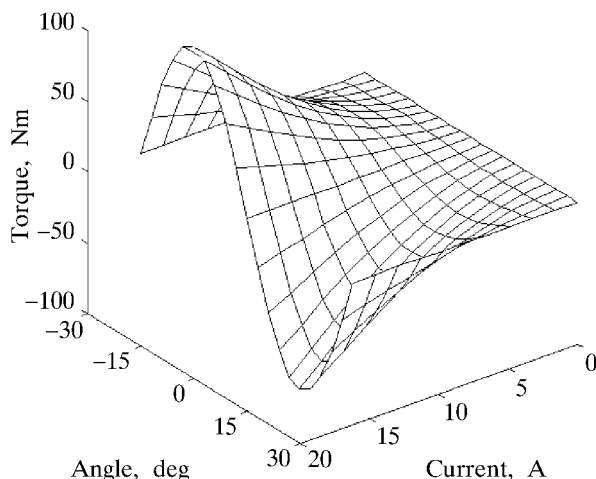


Fig. 10 Static torque $T(\theta, i)$

2 STEADY STATE CHARACTERISTICS

The steady state characteristics of the SR motor are computed with phase windings of the motor supplied from power electronic converter and for constant speed of rotation.

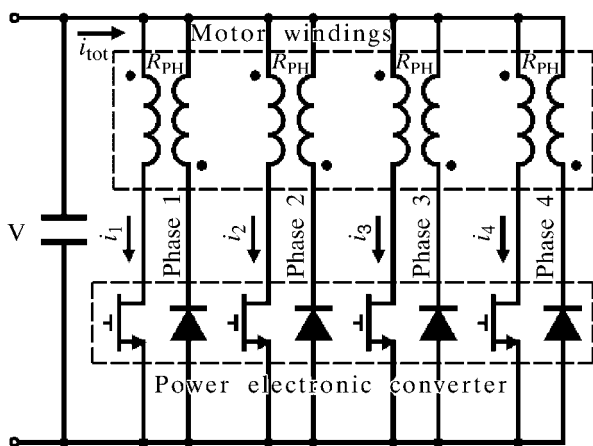


Fig. 11 Power electronic converter for SR motor with bifilar winding

An example of power electronic converter with only one witch per phase for the motor with bifilar windings is shown in Figure 11.

The basic equation for prediction of the quasi-static characteristics is:

$$\pm V = R_{1,2} \cdot i + \frac{d\Psi(\theta, i)}{dt} \quad (5)$$

where are: $\Psi(\theta, i)$ – flux linkage look-up table, V – voltage, R_1 is the resistance of the main phase winding (associated with $+V$) and R_2 is the resistance of the auxiliary phase winding (associated with $+V$), i – phase current.

The voltage has sign $\gg+\ll$ if switch is \gg switch-on \ll and sign $\gg-\ll$ if phase switch is \gg switch-off \ll . Commutation switching process in power electronic converter was negligible.

3.1 Current computation

The steady-state phase current value can be computed using voltage equation (5) in the form:

$$\frac{d\Psi(\theta, i)}{dt} = \pm V - R_{1,2} \cdot i \quad (6)$$

The method for computation of steady-state current from (6) is based on using nonlinear differential equations that do not require the evaluation of differential coefficients. The essential feature of the method is described in [8]. Here is given the brief outline of the method.

The given data defining the magnetic nature of the SR motor are stored in look-up table $\Psi(\theta, i)$ shown by diagram in Figure 8. The solution of equations (6) in the last form, to obtain current, requires definition of magnetic behavior of the motor in the form $i(\theta, \Psi)$ to enable the values of i to be updated after each step of numerical integration of the voltage equation (6) (i.e. after each integration step to find the corresponding current which is then inserted into right hand side of the voltage equation).

This look-up table $i(\theta, \Psi)$ is obtained by inverting the input table $\Psi(\theta, i)$. The intermediate values of $i(\theta, \Psi)$ required in the course of numerical integration are found by cubic interpolation both in θ and in Ψ .

The equation (6) are solved by the Runge Kutta 4th order integration method, the values of the flux linkage and current being found after each step of integration.

The steady-state waveforms of current and flux linkage are shown by diagram in Figure 12. The

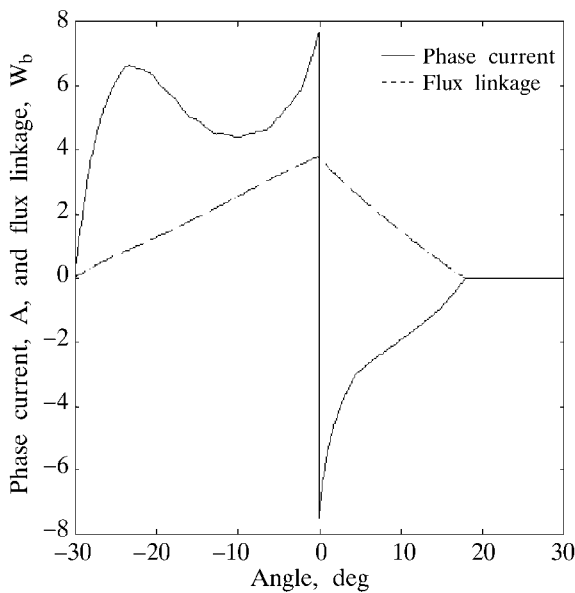


Fig. 12 Steady-state phase current and flux

current waveform in Figure 12 when switch phase is »switch-off« is showed with sign »-«.

3.2 Steady-state and average torque computation

The phase steady-state electromagnetic torque can be predicted from relation (4) with current calculated from relation (5). The total quasistatic torque is obtained by summing of the phase steady-state torque. Figure 13 and Figure 14 shows phase and total steady-state torque.

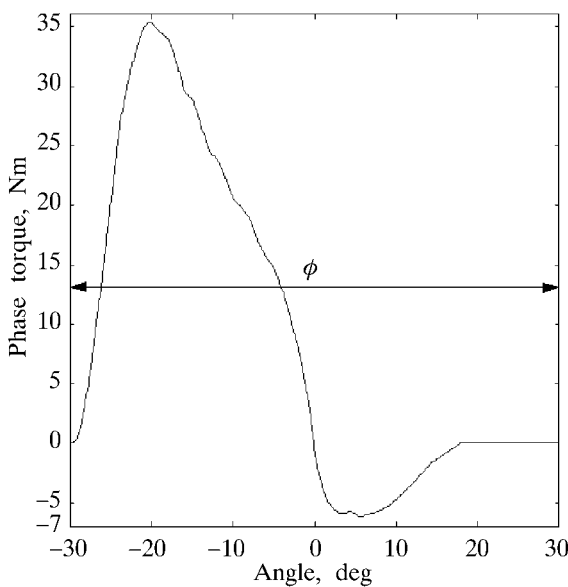


Fig. 13 Phase quasistatic torque

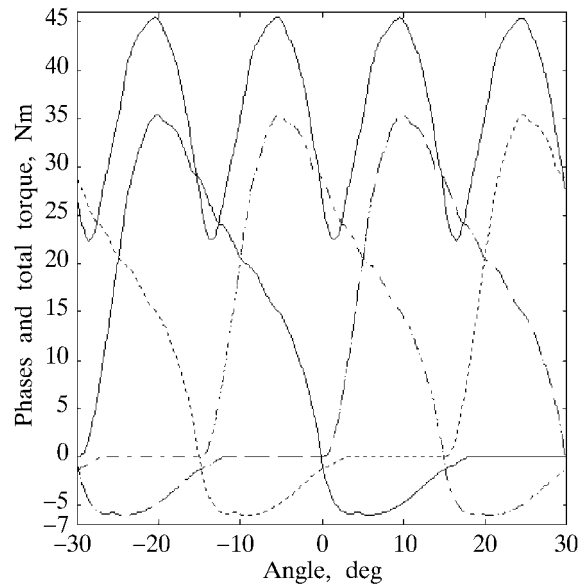


Fig. 14. Phases and total quasistatic torque

The average torque for one phase is given by:

$$T_{avg} = \frac{1}{\phi} \int_0^{\phi} T(\theta, i) d\theta = \frac{W_{co}}{\phi} = \frac{1}{\phi} \oint \Psi(\theta, i) di \quad (7)$$

where $\phi = 2\pi/N_R$ is angle of complete cycle of inductance (Figure 13).

As shown on the right hand side of Equation 7 the average torque can be also computed from the »energy conversion loop« which is described by the locus in the flux-linkage vs. current plane.

4 DYNAMIC CHARACTERISTICS

The mathematical model for predicting dynamic characteristics of SR motor is described by the following set of equations:

$$\begin{aligned} \frac{d\Psi_k(\theta_k, i_k)}{dt} &= \pm V - R_{1,2} \cdot i_k \\ \frac{d\omega}{dt} &= \frac{1}{J_I} \cdot \left[\sum_{k=1}^{n_{ph}} T_k(\theta_k, i_k) - T_L \right] \\ \frac{d\theta_k}{dt} &= \omega \\ \theta_k &= \theta_l + (k-1) \cdot \varepsilon, \end{aligned} \quad (8)$$

where are: ω – angular speed, T_L – load torque, ε – angular displacement between adjacent phases, J_I – moment of inertia, θ – rotor position, n_{ph} – number of phases of the motor.

This mathematical model enables computation of instantaneous values of phase and total currents and instantaneous value of phase and total torque and speed. The instantaneous total electromagnetic torque is obtained by summing instantaneous phase torque at instantaneous angular position. This value cannot be expressed analytically in terms of phase current, since magnetic saturation is present even at lower loading of the SR motor.

In computing procedure solving the equation of the mathematical model the look-up table of the flux linkage $\Psi(\theta, i)$ and torque $T(\theta, i)$ need to be known. These values are static characteristics of the SR motor and are obtained by static analysis.

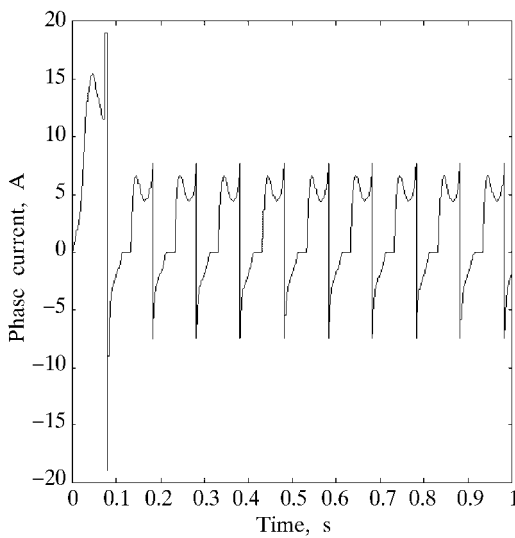


Fig. 15 Instantaneous phase current when the current limit is not activated

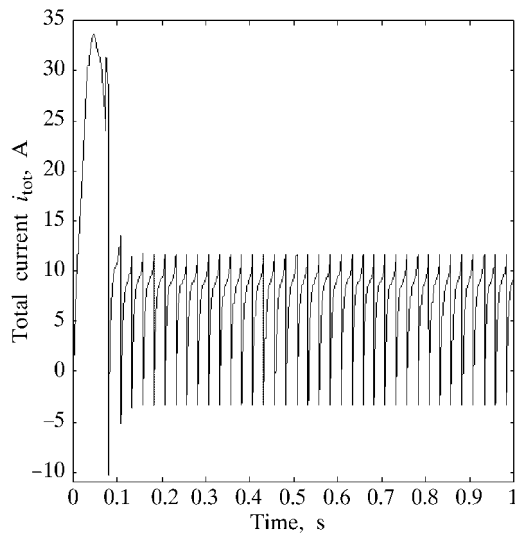


Fig. 16 Instantaneous total current

Rotor position sensing device gives information about rotor position (angle θ) in the control electronics block (Figure 1). The control electronic block defines the switching state for each phase i.e. the switch-on (θ_{on}) and switch-off (θ_{off}) angles. The voltage $+V$ is applied when $\theta_{off} \geq \theta > \theta_{on}$ and the voltage is $-V$ when $\theta \geq \theta_{off}$. The phase currents of the motor were limited by chopping process.

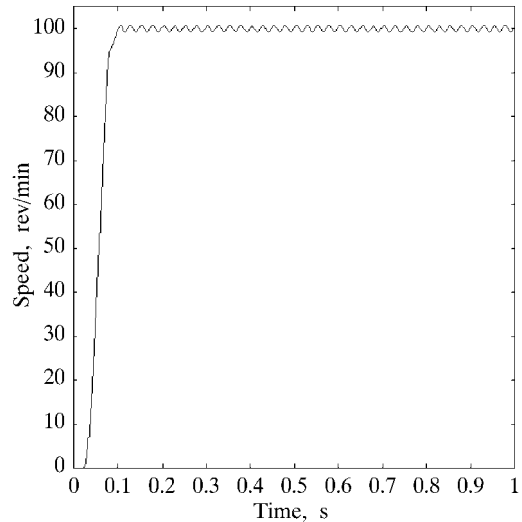


Fig. 17 Instantaneous dynamic speed

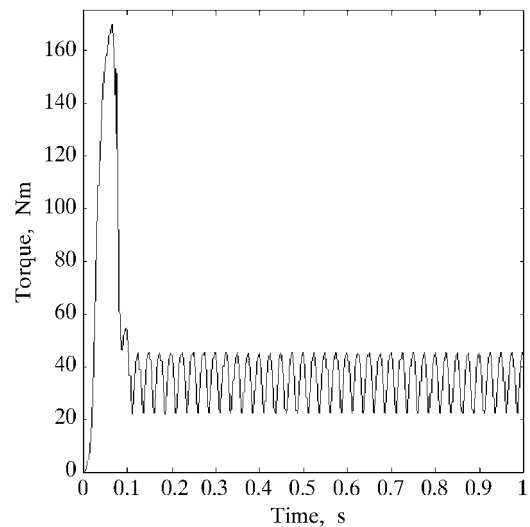


Fig. 18 Instantaneous dynamic torque

In the Figure 15, Figure 16, Figure 17 and Figure 18 are shown instantaneous values of the phase and total currents, total electromagnetic torque and speed for: $V = 105$ (V), $T_L = 36$ (Nm), $J_I = 10 \cdot J_M$ (kgm²), $\theta_{on} = -30$, $\theta_{off} = 0$.

5 EXPERIMENTAL RESULTS

A block diagram and a photograph illustrating measuring equipment are shown on Figure 19 and Figure 20. The SR motor was loaded with magnetic powder brake (Type: MOBAC, 6 (kW), 0–400 (Nm)).

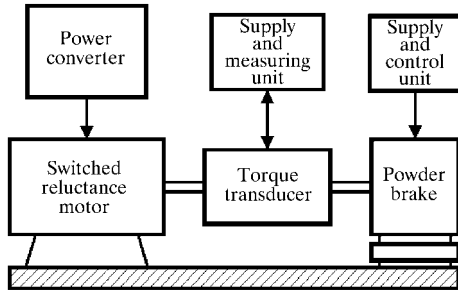


Fig. 19 Block diagram of experimental equipment

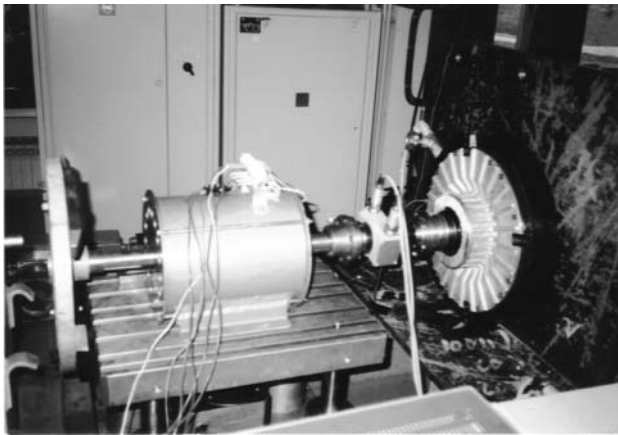


Fig. 20 SR motor and measuring equipment

Table 1 SR motor data

Stator poles	8
Rotor poles	6
Rated voltage (V)	150
Rated current (A)	6
Rated torque (Nm)	35.8
Rated power (kW)	0.75
Rated speed (rev/min)	200
Stator pole arc (°)	20
Rotor pole arc (°)	25
Stator outside diameter (mm)	240
Rotor diameter (mm)	139
Core length (mm)	190
Stator back of core width (mm)	17
Air gap (mm)	0.5
Practice coil area per pole side (mm)	463
Number of turns per phase winding	440
Type of winding	bifilar
Phase resistance (Ω)	3.52
Inertia torque (kgm ²)	0.057

The torque and speed were measured by a combined brushless type HBM-TSN200. On the other end of the shaft was added large rotational inertia so that speed ripple was negligible by measuring. The phase currents were measured by compensated Hall-effect current transducers and stored on a digital oscilloscope.

The flux linkage characteristics and static torque characteristic with blocked rotor were measured over an angular displacement θ in range from -30 to 0 in 3 increments and different excitation currents. In running conditions the motor was loaded by a magnetic powder brake.

Figure 21 and Figure 22 shows calculated and measured flux linkage and static torque.

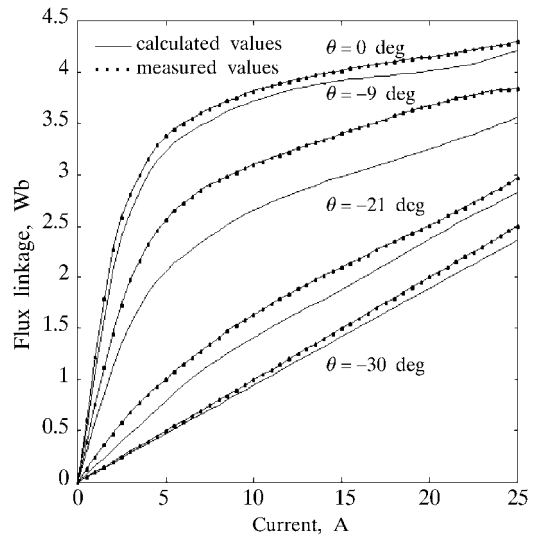


Fig. 21 Calculated and measured flux linkage $\Psi(\theta,i)$

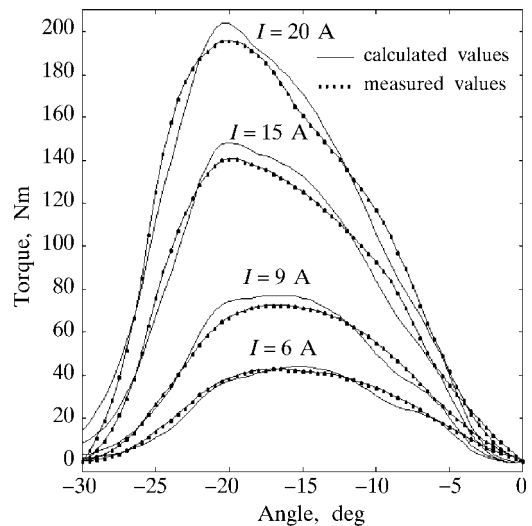


Fig. 22 Calculated and measured total static torque $T(\theta,i)$

Calculated and measured steady-state characteristics of phase current and total torque are shown in Figures 23–26, Figure 24, Figure 25 and Figure 26. These characteristics are obtained for $V=105$ (V), $T_L=36$ (Nm), $J_I=10 \cdot J_M$ (kgm²), $n=100$ (rev/min) (steady-state average speed), $\theta_{on}=-30$, $\theta_{off}=0$.

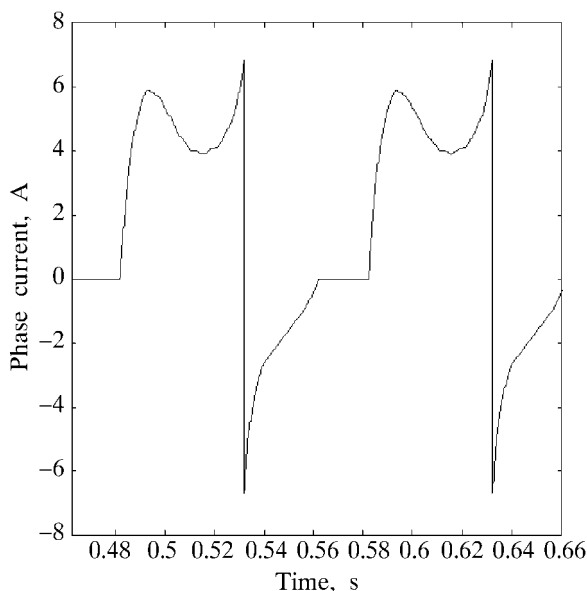


Fig. 23 Calculated steady-state phase current

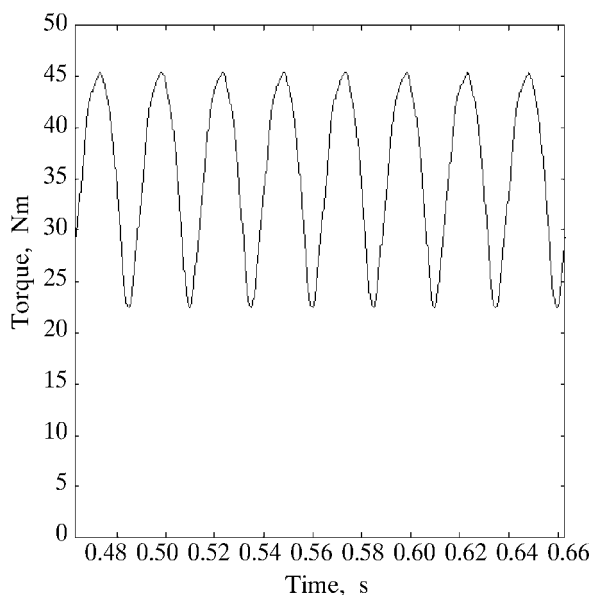


Fig. 25 Calculated total steady-state torque

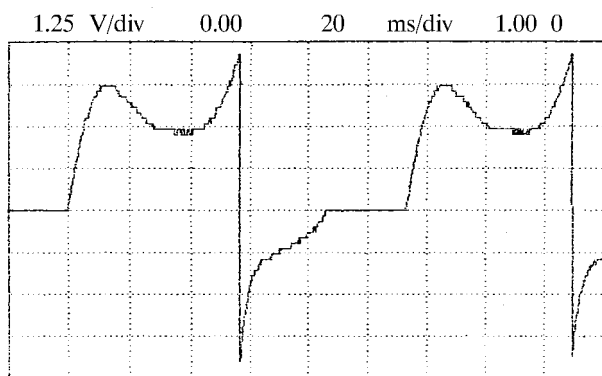


Fig. 24 Measured steady-state phase current, current scale: 1.25 (V/div)=2 (A/div), time scale: 20 (ms/div)

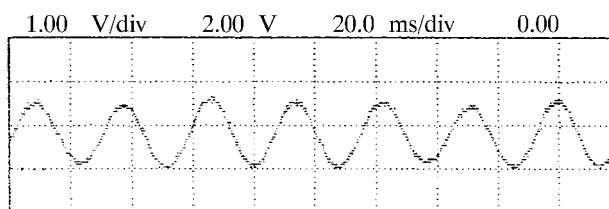


Fig. 26 Measured total steady-state torque, torque scale: 1.00 (V/div)=20(Nm/div), time scale: 20 (ms/div)

6 CONCLUSION

In the modelling procedure the SR motor is described by static flux-linkage vs. current characteristics for set of angles from fully misaligned to fully aligned position. These characteristics are obtained from the machine physical parameters (dimensions, number of turns and B-H characteristic) by means of magnetic field analysis, and are in general non-

linear and non-sinusoidal. Using the set of these magnetization characteristics, as a look-up table, the set of static coenergy and torque characteristics are obtained by applying numerical integration and differentiation.

In a steady-state operation, when the machine speed is assumed constant, it is sufficient to solve only voltage equation of one phase to obtain the phase current and torque waveform. The total torque waveform is obtained by adding the appropriately shifted phase torque waveforms.

In dynamic conditions, when the speed is not constant, all phase equations must be solved simultaneously together with mechanical equations to obtain instantaneous current and torque characteristics. The described model represents the SR machine with good accuracy for a variety of operating conditions in which the machine does not produce significant core losses.

REFERENCES

- [1] P. J. Lawrenson, P. J. Stephenson, P. T. Blenkinsop, J. Čorda, N. N. Fulton, **Variable-speed Switched Reluctance Motors**. IEE proceedings vol. 128, Pt B, no. 4, pp. 253–265, July 1980.
- [2] T. J. E. Miller, **Switched Reluctance Motors and their Control**. Clarendon Press, Oxford, 1993.
- [3] W. F. Ray, R. M. Davis, **Inverter Drives for Doubly Salient Reluctance Motor: its Fundamental Behavior, Linear Analysis and Cost Implications**. Electric Power Applications, vol. 2, no. 6, pp. 185–193, December 1979.
- [4] R. M. Davis, W. F. Ray, R. J. Blake, **Inverter Drive for Switched Reluctance Motor**. IEE proceedings vol. 128, Pt B, no. 2, pp. 126–136, March 1981.
- [5] J. T. Bass, M. Ehsani, T. J. E. Miller, **Robust Torque Control of Switched Reluctance Motor without a Shaft Position Sensor**. IEEE Transactions, vol. IE-34, May 1987.
- [6] M. R. Hariss, J. W. Finch, J. A. Mallick, T. J. E. Miller, **A Review of the Integral-horsepower Switched Reluctance Motor Drive**. IEEE Transactions, vol. IA-22, July/August 1986.
- [7] R. Arumugam, D. A. Lowter, R. Krishanan, J. F. Lindsay, **Magnetic Field Analysis of a Switched Reluctance Motor Using a Two Dimensional Finite Element Model**. IEEE Transaction on Magnetics, vol. MAG-21, no. 5, September 1985.
- [8] J. M. Stephenson, J. Čorda, **Computation of Torque and Current in Doubly Salient Reluctance Motors from Nonlinear Magnetization Data**. Proceedings IEE, Vol. 126, No. 5, May 1979, pp. 393–396.
- [9] J. Čorda, Š. Mašić, J. M. Stephenson, **Computation and Experimental Determination of Running Torque Waveforms in Switched-reluctance Motors**. Proceedings IEE-B, vol. 140, no. 6, November 1993.
- [10] Š. Mašić, **Minimizacija pulzacija momenta prekidačko-reluktantnog motora kod niskih brzina rotacije**. Ph D Thesis on Faculty of Electrical Engineering Sarajevo, 1992.

Proračun statičkih, kvazistatičkih i dinamičkih karakteristika prekidačko-reluktantnog motora. Rad opisuje postupke proračuna statičkih karakteristika (ulančeni tok, magnetska koenergija i moment), kvazistatičkih karakteristika (brzina i moment) i dinamičkih karakteristika (brzina, struja i moment) prekidačko-reluktantnog motora. Raspodjela magnetskog vektor potencijala na poprečnom presjeku motora računata je metodom konačnih elemenata. Ulančeni tok, induktivnost, magnetska koenergija i statički moment računati su za različite pozicije rotora i struje statora. Kvazistatičke i dinamičke karakteristike su računane pomoću posebno razvijenih programa u programskim jezicima Fortran 77 i Matlab/Simulink. Svi proračuni provedeni su za prekidačko-reluktantni motor sa 8 polova statora i 6 polova rotora. Rezultati proračuna su potvrđeni eksperimentom.

Ključne riječi: prekidačko-reluktantni motor, karakteristike, modeliranje

AUTHORS' ADDRESSES:

Dr Šemsudin Mašić
Department of Electrical Machines and Drives
Faculty of Electrical Engineering on Sarajevo
Zmaja od Bosne bb, 71000 Sarajevo
Bosna and Hercegovina
E-mail: smasic@utic.net.ba

Dr Jasmin Čorda
Senior Lecturer and Mechatronic Course Tutor
Department of Electronic and Electrical Engineering
University of Leeds
Leeds LS2 9JT
E-mail: j.corda@elec-eng.leeds.ac.uk

Senad Smaka
Department of Electrical Machines and Drives
Faculty of Electrical Engineering in Sarajevo
Zmaja od Bosne bb, 71000 Sarajevo
Bosna and Hercegovina
E-mail: ssmaka@utic.net.ba

Received: 2002–07–12